2001

Two Photon Absorption in Chromophore Doped Solid Matrices

Stefan Mancas
University of Central Florida, mancass@erau.edu

Michael Canva

Yves Levy

Kathleen A. Richardson

Giselle Roger

Two Photon Absorption in Chromophore Doped Solid Matrices

Stefan Mancas
University of Central Florida

IOTA Dr. Michael Canva
IOTA Dr. Yves Levy
CREOL Dr. Kathleen A Richardson
IOTA Giselle Roger

Abstract

Over the past decades organic materials have shown an important potential for applications in the field of nonlinear optics. Two-photon absorbing materials can be optically addressed in three dimensions of space, which make them unique for many new applications, including 3D displays, optical memories, bio-sensors, etc. Fluorescent organic chromophores can be synthesized with structures especially optimized for this nonlinear optical property. Yet, for some applications, they have to be incorporated in solid state matrices.

We especially investigate hybrid organic/inorganic doped matrices synthesized by sol-gel process. However , the linear transmission for such molecules is often significantly less than unity. Two-photon absorption (TPA) offers the advantage of very high transmission at low incident intensity, while being sensitive to high intensity laser pulses.

Our aim is to record a 3D layered pattern of optical memory inside the sample by the use of the picosecond pulsed ND^{3+}:YAG laser at 532nm, or 1064nm.

Introduction

In the presence of intense laser pulses, molecules can simultaneously absorb one, two or more photons, and the transition probability for absorption of two identical photons is proportional with I^2, where I is the intensity of the laser pulse.

Photons are absorbed in a solid through a process known as the photoelectric effect. A photon interacts with an electron by giving all its energy to the electron. The absorption of photons in solids depends on the number of electrons that can accept a transfer of energy from the photon. Not all electrons meet this criterion. Some electrons are so tightly bound to their orbital around the atomic nucleus that the photon energy is unable to break the bonds. Other electrons are involved in the bonding between atoms and cannot be freed by the energy of the incident photons. For example, ordinary window glass is transparent to visible photons, but is strongly absorbent to ultraviolet radiation where the photons have energies only a few times greater than that of visible light.

The mechanism for absorption is that a photon transfers all its energy to an electron in the absorbing material. The photon is "lost" from the light beam as it is absorbed in a single event. As you can see from the **Figure I** the electron is excited by the gain in energy to a higher energy state in the electron configuration around the atom. This single-event transfer of photon energy to an electron and the disappearance of the photon is closely related to the photoelectric effect where the electron is ejected from the material in a single event. The

electron is ejected from the atom by the absorption of an x-ray. This loss of an electron leaves the atom in an excited state.

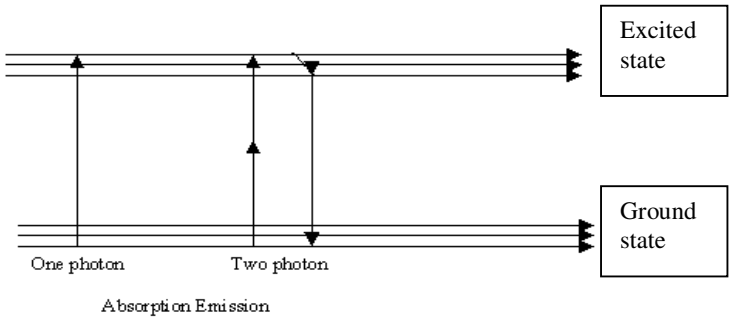

Figure I Schematic mechanism for one and two photon absorption and emission

TPA (two photon absorption) will take place only if the energy of the two photons corresponds to the energy absorbed by the dye. From **Figure II** the sources are chosen so twice the energy of the neither source lies in the dye solution's absorption band but the sum of the energies of a single photon does.

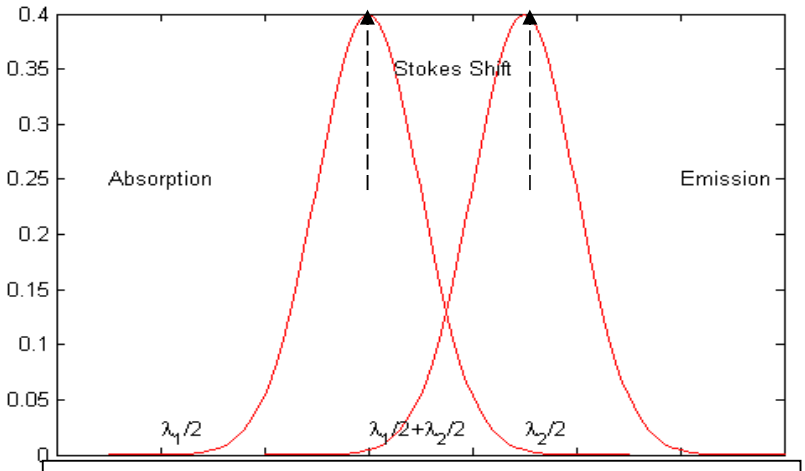

Figure II Absorption and emission vs. wavelength

One photon absorption is a very efficient process but two photon absorption is only occurring at very high intensities by two techniques as you can see from **Figure III.** Both techniques show optical 3D special addressing:

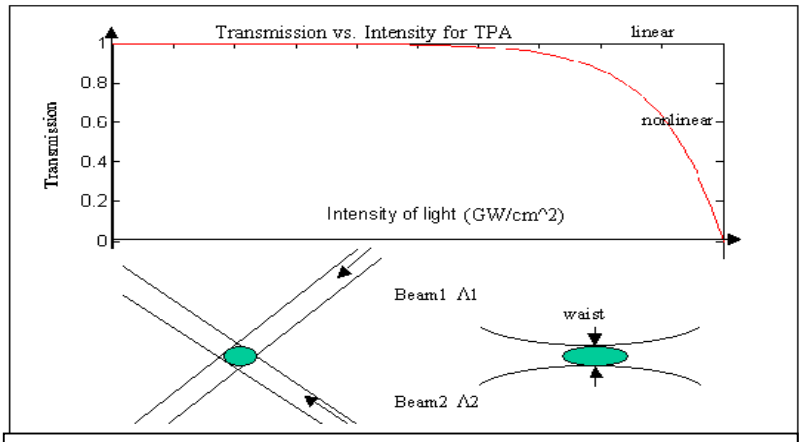

Figure III Techniques for showing TPA
a)By crossing the light
b)Two powerful beams of different wavelength

Future Applications of TPA

TPA permits the fabrication of 3D structures and the definition of lithographic features on non planar surfaces such as two photon fluorescence imaging and 3D optical data storage. Molecules exhibiting strong TPA hold great potential for a wide range of applications. The fabrication of complex 3D structures by TPA is demonstrated and discussed in the context of advanced photonic applications.

3D addressing is a future technique and is due to nonlinear interactions. Since the two-photon absorption is confined to a tiny volume at the focus of the laser, 3D polymer patterns can be produced by scanning the focus within the material.

3D Optical storage memories

A new 3D optical memory **Figure IV** device will allow fast random access of the information and extremely high bit densities. The device will be based on the two-photon writing, reading, and erasing the information in a photochromic material embedded in a polymer matrix. Such a 3D optical memory will be based on volume and erasable optical storage in an amplitude recording medium. Replacing lenses with holographic gratings allows parallel addressing.

This method is based on a virtual two-photon process in which neither of the two photons can be absorbed individually: both must be absorbed simultaneously, which necessitates that the two beams overlap in time and space within the 3D medium. Advantages are: immense information storage capacity (10^{12} bits/cm^3), random access, parallel addressing, very fast optical writing and reading speeds.

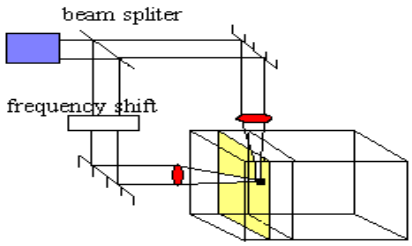

Figure IV Schematic diagram of a 3D optical memory based on TPA

3D Displays

3D perception is a complex cognitive process involving the eyes and the brain as a visual system. Historical solutions are diverse and varied and often relied on thinking that human visual system is a 2D scene with the perception of depth. Although specific system requirements vary for different applications, a successful 3D display will provide the viewer with a number of intrinsic visualization parameters. These parameters include the field of view, and the viewing zone. This will offer a valuable approach for presenting real-time multidimensional information to a multitude of viewers independent of viewing perspective, with no obstructed viewing regions and no need for special viewing eyewear.

The physical mechanism on which this 3D display technology is based is known as two-step, two-frequency upconversion. This phenomenon occurs when an active ion that has been doped in small quantities into a bulk transparent host material is optically excited to higher energy levels by absorbing energy from two different wavelength near IR beams. The active ion which occupies the lower energy E0 can absorb energy from the first IR beam of wavelength λ_1 making transition to intermediate excited state E1 where it will stay for the lifetime τ of this level. If the second IR beam impinges on this ion while it is in the first excited state, it will absorb energy at the second laser wavelength λ_2 and undergo a transition to the excited state E2. An ion that has been excited in this manner has effectively summed the energy it absorbed from both pump photons and can re-emit most of it as a single photon of visible light by decaying back to the ground state **Fig V a**.

It is crucial that the excitation process in the active ion occurs only from the selective absorption of two different IR wavelengths. By controlling the spatial coordinates of the intersection of the two lasers one can address a volumetric pixel at a specific location inside the bulk medium **Fig V b.**

Rapidly scanning the point of intersection inside the display volume, moves the position of the pixel and allows 3D images to be drawn.

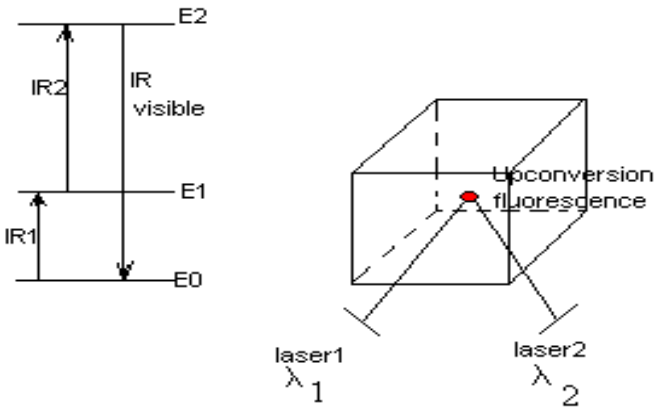

Figure V a) Energy level diagram of an active ion
b) Two scanned intersecting beams to address and draw objects in a transparent material doped with an active ion

Setup

In our experimental setup we used an incident high power laser beam from a Q switched neodymium-doped yttrium aluminum garnet ND^{3+}:YAG pumped laser with a wavelength of 532nm, or1064nm, repetition rate of 10Hz, and pulse of about 0.5ps.

A neutral density filter set and a focusing lens were placed in the optical path of the incident beam before our sample. The local intensity of the incident laser beam could be controlled by changing the combinations of the densities filters.

The position of the sample could also be smoothly varied along the z-axis so the local intensity within the sample could be changed under a total incident laser power level.

A beam splitter was inserted into the beam path to provide an incident intensity reference (Channel 1), as you can see from the **Figure VI.**

The transmitted laser beam from the sample is recorder by photo-detectors and transmitted through an oscilloscope and using a GPIB interface to a data acquisition computer. TPA could be measured directly from beam attenuation if the absorption is sufficiently strong.

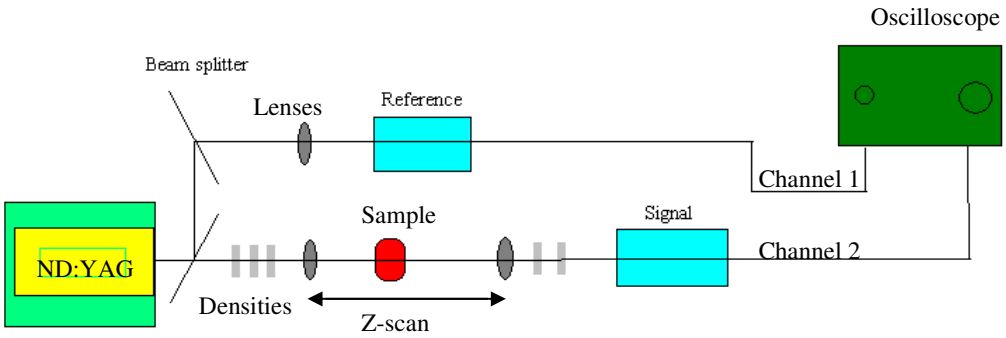

I=E/(p*S)
1) move densities [changing I]
2) move the sample along the z axis [changing S]

where: I-intensity of light in GW/cm^2
E-incident energy in mJ
S-surface area in cm^2
p-pulse duration in ps

Figure VI Experimental setup

Derivation based on a modified Beer Lambert Law

In spite of the different material dependencies in the description of visible light and x-ray absorption, the mathematical description is the same for the two: the exponential decay law. This decay law is due to the fact that each successive interval of equal thickness of a sample absorbs an equal fraction of the photons passing through it. Each successive interval, however, receives fewer photons than the preceding interval because the number of photons decreases with depth as you can see from the **Table I.**

layers	**Incident on layer**	**Absorbed in layer**	**Transmitted through layer**
1	I	I*A	I*(1-A)
2	I*(1-A)	I*A*(1-A)	I*(1-A)exp(2)
3	I*(1-A)exp(2)	I*A*(1-A)exp(2)	I*(1-A)exp(3)
.			
.			
.			
n	I*(1-A)exp(n-1)	I*A*(1-A)exp(n-1)	I*(1-A)exp(n)

Table I Transmission for an absorbed fraction A

For n layers, the total absorption T_A in all layers absorbed fraction A will be

$$T_A = I(A + A(1-A) + A(1-A)^2 + \ldots + A(1-A)^{n-1})$$

$$T_A = \sum_{k=1}^{n} IA(1-A)^{k-1} = AI\sum_{k=1}^{n}(1-A)^{k-1} = AI\sum_{k=0}^{n}(1-A)^{k}$$

$$T_A = AI\frac{(1-A)^{n+1}-1}{(1-A)-1} \Rightarrow T_A = I(1-(1-A)^{n+1})$$

if $0<A<1 \Rightarrow 0<1-A<1 \Rightarrow$ the series converges to *I*. That would be a case when the material would absorb all the incident beam (or the transmission will be 0).

The Beer-Lambert law can be derived from an approximation for the absorption coefficient for a molecule by approximating the molecule by an opaque disk whose cross-sectional area σ represents the effective area seen by a photon of frequency υ, as you can see in the **Figure VII.** Taking an infinitesimal slab, $d\tau$. of sample where:

I_o is the intensity entering the sample at z=0,
$I\tau$. is the intensity entering the infinitesimal slab at z,
dI is the intensity absorbed in the slab, and
I is the intensity of light leaving the sample,
N is the number of molecules/cm^3
S is total area in cm^2

$\Rightarrow$ the total opaque area on the slab due to the absorbers is $\sigma * N * S * d\tau$.

$\Rightarrow$ the fraction of photons absorbed will be $\dfrac{\sigma * N * S * d\tau}{S}$

so,

$$dI / I\tau. = -\sigma * N * d\tau.$$

$$\int_{\tau=0, I=I_0}^{z, I=I} dI / I_\tau = \int_{\tau=0}^{z} -\sigma * N * d\tau$$

$$ln(I) - ln(I_o) = - \sigma * N * z$$

or

$$-\ln(I / I_o) = \sigma * N * z$$

Let

$$c\frac{moles}{L} = N\frac{molecules}{cm^3} * \frac{1mole}{6.023*10^{23} molecules} * \frac{10^3 cm^3}{L}$$

where c is the concentration in moles/L

And

$$lnx=ln(10)*log(x)$$

Then

$$-\log(\frac{I}{I_0}) = \frac{\sigma * 6.023*10^{20}}{\ln 10} * c * z$$

Or

$$-log(I/I_0)=A=\varepsilon*c*z$$

Where

$$\varepsilon=\sigma*2.61*10^{20}$$

Experimental measurements are usually made in terms of transmission *(T),* which is defined as:

$$T = I / I_o$$

The relation between *A* and *T* is:

$$A = -log\ T = -\ log\ (I / I_o)$$

In the presence of one and TPA described by the absorption coefficients α (attenuation coefficient due to linear absorption and scattering) and β (nonlinear absorption coefficient due to TPA), the change in intensity of light as it passes through the sample is given by:

$$\frac{dI}{dz} + \alpha I + \beta I^2 = 0$$

The solution of this differential equation is:

$$I(z) = \frac{I_0 * e^{-\alpha * z}}{1 + \frac{\beta}{\alpha} * z * I_0 - \frac{\beta}{\alpha} * I_0 * e^{-\alpha * z}}$$

In the case of small linear absorption α*z<<1
The solution becomes

$$I(z) = \frac{I_0 * e^{-\alpha z}}{1 + \beta * z * I_0}$$

And the transmission of the nonlinear medium through sample can be written as:

$$T(z) = \frac{I(z)}{I} = \frac{e^{-\alpha * z}}{1 + \beta * z * I_0} = \frac{T_0}{1 + \beta * z * I_0} = T_0 * T_i$$

Where:

T_0 is the linear transmission (independent of I_0)
T_i is the nonlinear transmission (dependent of I_0)

If the beam is focussed near the sample and a Gaussian distribution can be assured, the nonlinear transmission T_i can be modified as:

$$T_i = \frac{\ln(1 + I_0 * \beta * z)}{I_0 * \beta * z}$$

If the nonlinear transmission change is due only to the TPA process, according to the theory the nonlinear absorption coefficient β should be independent of the input intensity I_0 for a given sample.

All these equations were implemented in the Matlab program and also were used by the Igor Pro software for calculation of transmission.

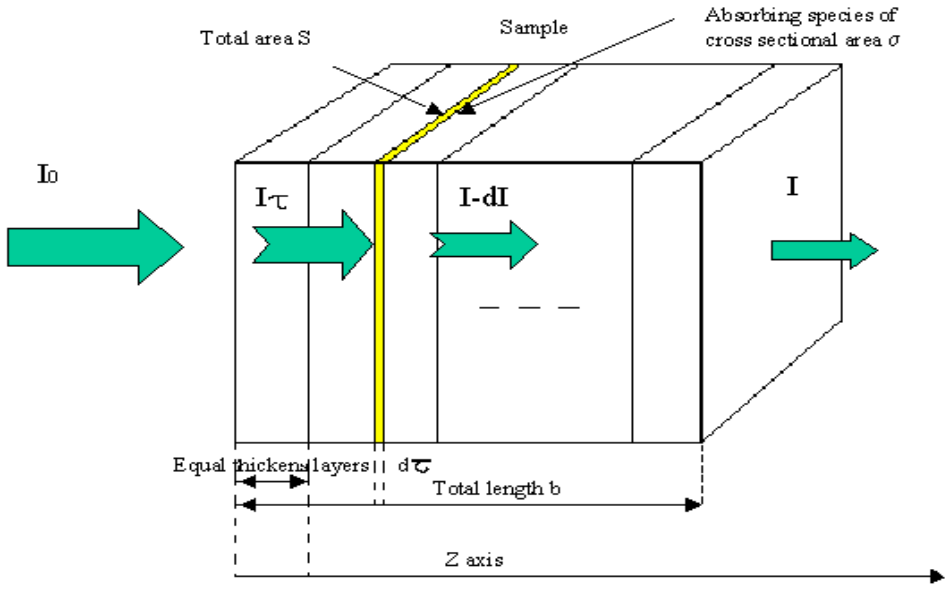

Figure VII Explanation of Beer Lambert Law

Graphs and Results

In my first part of the experiment we used the visible green 532nm of the ND^{3+}:YAG laser with a frequency of 10Hz.

Sample (perryorange $2*10^{-4}$) is positioned along the axis of a focussed high intensity beam so that the focal point could be scanned through one side of the sample. This results in a position dependent attenuation of the beam which allows the nonlinear loss to be measured when the full transmitted beam is collected. Under the excitation of 532nm laser beam, beam size of 4 mm and a repetition rate of 10 Hz, I could not notice TPA. The transmission vs. Intensity for perryorange at 532nm can be seen in the **Appendix** in **Figure VIII.** All data that was obtained and calculated can be seen in the **Table VIII**. All acquisitions were done using a Macintosh computer and the software IGOR Pro. Using an old program I designed and improved it to automatically permit the calculation of transmission when changing the input intensity. All acquisitions from the reference beam and the signal beam were done using the sensors that were connected to an oscilloscope that had the output the reference and signal voltages. The densities for 532nm were changed using the following pattern from **Table II**

Densities utilised for a wavelength of 532nm								
No	**Density**	**0.15G**	**0.3G**	**0.6G2**	**1G2**	**1.3G**	**1.3G2**	**1.6G2**
0	6.294	+	+	+	+	+	+	+
1	6.138		+	+	+	+	+	+
2	5.995	+		+	+	+	+	+
3	5.696	+	+		+	+	+	+
4	5.278	+	+	+		+	+	+
5	4.975	+	+	+	+		+	+
6	4.705	+	+	+	+	+	+	
7	4.406	+		+	+	+	+	
8	3.959	+	+	+			+	+
9	3.689	+	+	+		+	+	
10	3.39	+		+		+	+	
11	3.087	+		+	+		+	
12	2.792	+				+	+	
DOTotal=8.9 with 1G2 and 1.6G2 in front of the detector on reference channel								

Table II Densities utilized for 532nm
+ means incident density(the density in the front of sample)

Then we changed the setup and used the invisible wavelength of 1064nm. We also changed the sample, now we used (pyrro 605 $5.5*10^{-4}$). Here we noticed interesting things. After we calibrated the sensor, and changing the input intensity by changing the densities according to the pattern from the **Table III**, fluorescence emission induced by TPA can be easily observed. We obtained a very nice curve Transmission vs. Intensity for the pyrro605 at 1064nm. The results can be seen in **Figure IX, Table IX** of the **Appendix**.

Densities utilised for a wavelength of 1064nm									
No	Density	micro blade	blade 1	0.15G	0.15G2	0.3G	0.6G	1.0G	2.3G
0	4.434	+	+	+	+	+	+	+	+
1	4.161	+	+		+	+	+	+	+
2	3.781	+	+	+	+		+	+	+
3	3.507	+	+		+		+	+	+
4	3.234	+	+				+	+	+
5	2.967		+	+	+	+	+	+	
6	2.694		+		+	+	+	+	
7	2.481	+	+			+	+	+	
8	2.260			+	+	+		+	
9	2.121	+				+			+
10	1.969	+	+	+	+	+	+		
11	1.820			+	+	+	+		
12	1.695	+	+		+	+	+		
13	1.546				+	+	+		
14	1.393	+		+				+	
15	1.272					+	+		
16	1.148		+					+	
17	1.059							+	
18	0.928				+	+			
19	0.802	+	+			+			
20	0.654					+			
DOTotal=6.12 with 1G2 and 0.6G2 in front of the detector on reference channel									

Table III Densities utilized for 1064nm
+ means incident density(the density in the front of sample)

The values of the densities that we utilized are found in **Table IV**

density value	measured value	
	532nm	1064nm
0.15	0.156	0.274
0.15G2	0.158	0.272
0.3	0.299	0.654
0.6	0.588	0.618
0.6G2	0.598	0.633
1.0	1.014	1.059
1.0G2	1.016	1.055
1.3	1.319	1.395
1.3G2	1.317	1.393
1.6G2	1.589	0.995
2.0	2.036	1.272
2.3	2.239	1.407
2.3G2	2.245	1.428
2.6	2.544	1.587
2.6G2	2.557	1.595
microblade		0.06
blade 1		0.0886

Table IV The values of the densities that we utilized for both 532nm and 1064nm

The third part of the experiment was to try to do a Z-scan. In the Z-scan the same sample is positioned on a 3D support that will permit moving it in the (x,y) directions and along the beam (z direction). By looking at the graph from **Figure IX** one could choose an input intensity by choosing the corresponding density to obtain a Z-scan. The result of the Z-scan for the pyrro605 can be seen in the **Figure X, Table X** of the **Appendix.** Between 14 and 16 mm I also have taken more data to have a precise measurement as you can see in **Figure XI, Table XI** of the **Appendix.**

To make sure it works we repeated the experiment using the same sample that we used at 532nm (perryorange $2*10^{-4}$). The results can be seen the **Figure XII, Table XII** of the **Appendix.** By choosing again a desired input intensity we also made a Z-scan for the same sample using a constant density. The results that can be seen in **Figure XIII** and **Table XIII** of the **Appendix.**

We monitored higher order contributions due to the nonlinear absorption by employing different input energies to obtain a series of z-scans.

The most important and interesting part of my experiment was trying to inscribe the points in the sample for the optical memories. For inscribing points volumetric I used the following pattern where you can see it in the **Figure XIV.**

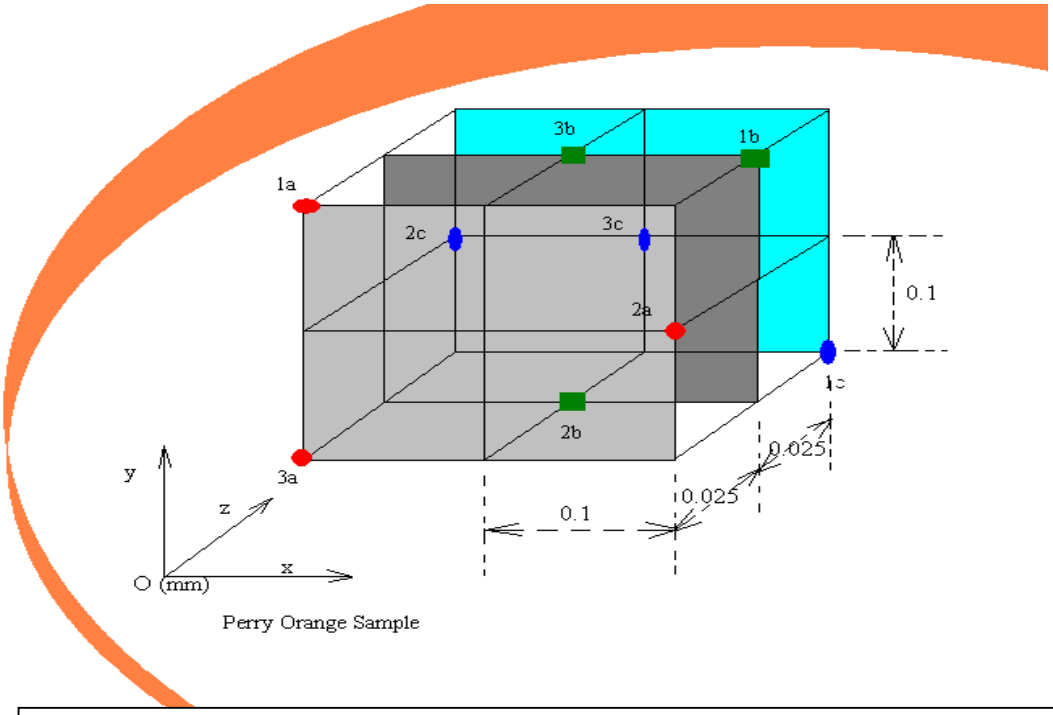

Figure XIV Inscribing nine points in three different planes in the perryorange sample

Using the same sample, and keeping a constant densities, I varied my sample along xyz directions to record the pattern from the figure. I tried to inscribe nine points at different positions, three in each layer for three layers. The surface points were 1a,2a,3a. Then I moved my sample 0.025mm along z and recorded another three set of pints 1b,2b,3b, then again moved the sample for another 0.025mm and record the last three points 1c,2c,3c. The distance between the points was 100µm (or 0.1mm), respective 200µm. The coordinates of the points can be seen in **Table V**.

The coordinates of the inscribed points			
first plane (a)	**x**	**y**	**z**
1a	8.9	7.0	15.95
2a	9.1	6.9	15.95
3a	8.9	6.8	15.95
second plane (b)			
1b	9.1	7.0	15.975
2b	9.0	6.8	15.975
3b	9.0	7.0	15.975
third plane (c)			
1c	9.1	6.8	16.0
2c	8.9	6.9	16.0
3c	9.0	6.9	16.0

Table V The coordinates of the inscribed points

Then we took the sample and analyzed with white light. We tried a scanning in depth to see and the pattern we recorded. The 3Dscan can be seen in **Figure XV.**

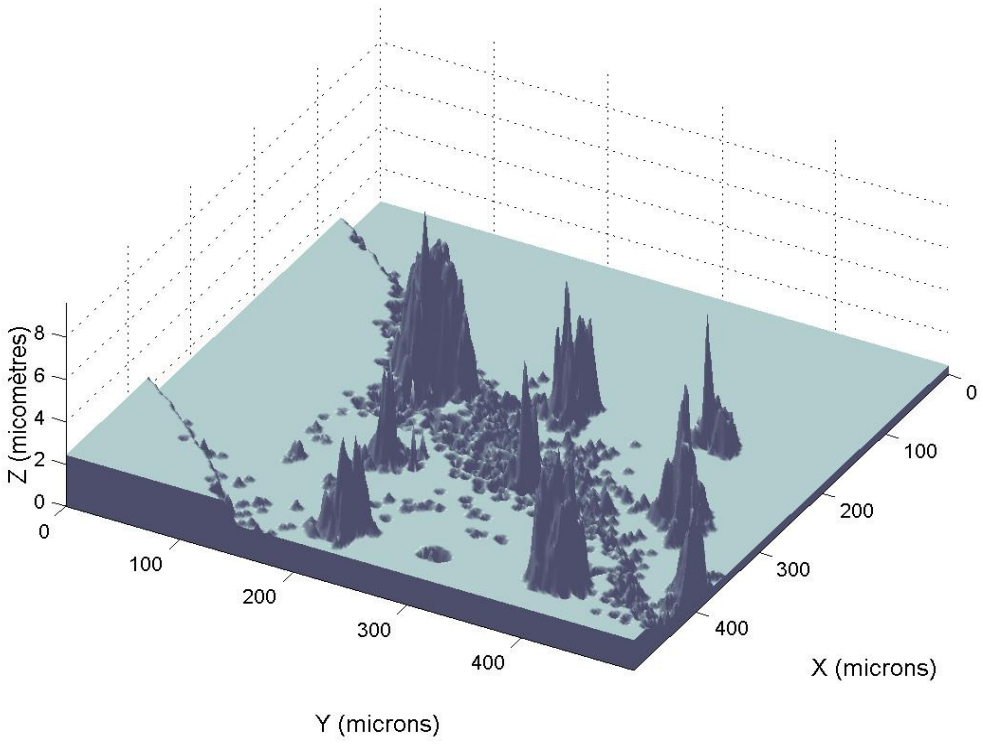

Figure XV 3D scan of the pattern presented in **Figure XIV**

The next graphs show all the nine points recorded at different depths in the material:

5,6 and 7 are the graphs which show the points on the surface, 8,9 and10 are on the second layer; 11,12 and respectively 13 the third layer.

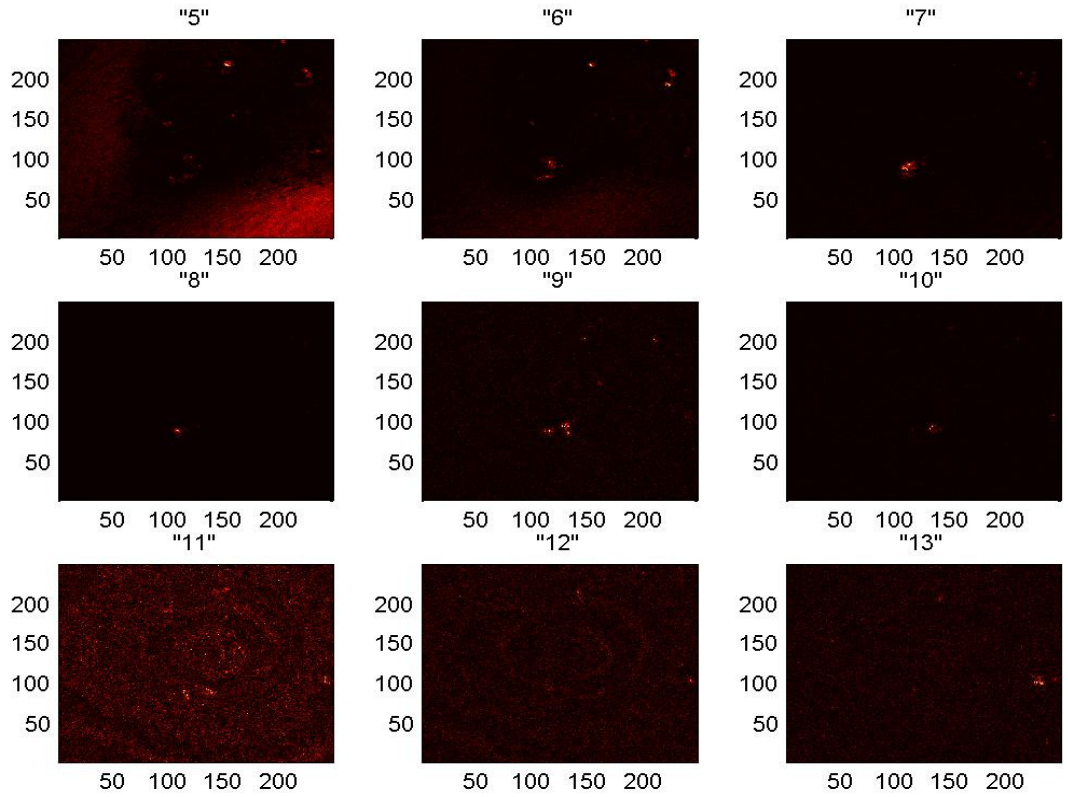

Figure XVI In depth scan that shows where the inscribed points are

The values of the intensity and the transmission graph for inscribing points into the sample can be seen in **Figure XVII** and the data in **Table XVII** of the **Appendix.**

Conclusion

We have presented results obtained with perryorange $2*10^{-4}$ and pyrro605 $5.5*10^{-4}$, and show that these kind of samples exhibit large two-photon absorption as determined by using the 1064nm ND:YAG pumped dye-laser and the picosecond pulses. The studies suggest that two-photon induced excited-state absorption contributes to the large effective two-photon absorptivities, and by controlling the position of the two-photon resonance, it is possible to have strong nonlinear absorption over much of the visible spectrum while also maintaining high linear transmission.

Samples similar with ours should greatly facilitate a variety of new applications of two-photon excitation in biology, chemistry, medicine, photonics, material science, optical limiting, computers, 3D displays, 3D memories, bio-sensors, etc.

Acknowledgments

This summer research program REU (Research Experiences for Undergraduates in Lasers and Optics) was possible due to collaboration between CREOL (School of Optics from University of Central Florida) and IOTA(Ecole Supérieure d'Optique/Insitut d'Optique) and was sponsored by CREOL and NSF. Special thanks to my advisor from IOTA Dr. Michael Canva, and also the advisor from CREOL Dr. Kathleen A Richardson. I also want to mention other people that participated in this program: from IOTA Dr.Yves Levy, Dr. Marc Bondiou, the Ph.D. student that helped me setting up the experiments Giselle Roger; from UCF Dr. Madi Dogariu and Dr. Bhimsen Shivamoggi and from ESPCI (Ecole Supérieure de Physique et de Chimie Industrielles) Benoit Forget and François Ramaz part of the photorefractive materials group.

References

1.Wavemetrics Inc., "IGOR Pro programming and reference manual", **Vol. 3**,(1996)
2.James H. Strickler and Watt W.Webb," Three-dimensional optical data storage in refractive media by two-photon point excitation",**Vol.16**,(1991)
3.Elizabeth Downing, Lambertus Hesselink, John Ralston, Roger Macfarlane, "A three-color, solid-state, three-dimensional display", **Vol. 273**, (1996)
4.Dimitri A. Parheneopoulos, Peter M. Rentzepis, "Three-dimensional optical storage memory", **Vol. 245**, (1989)
5.Guang S.He, Lixiang Yuan, "Nonlinear optical properties of a new chromophore", **Vol.14**, (1997)
6.Germain Puccetti, Simon G. Bott, Roger M. Leblanc, "Efficient two-photon –induced fluorescence in a new organic crystal", **Vol. 15**, (1998)
7.Alexandra Rapaport, Karine Ayrault, Eyitope St. Matthew-Daniel, and Michael Bass, "Visible light emission from dyes excited by simultaneous absorption of two different frequency beams of light", **Vol. 74**, (1999)
8.Marius Albota, David Beljone, "Design of organic molecules with large two-photon absorption cross sections", **Vol. 281**, (1998)
9.E.Ehrlich, X.L.Wu, "Two-photon absorbing organic chromophores for optical limiting", **Vol. 479**, (1997)
10.Guang S.He., Gen C. Xu, Paras N. Prasad, " Two-photon absorption and optical-limiting properties of novel organic compounds", **Vol. 20**, (1995)

Appendix